

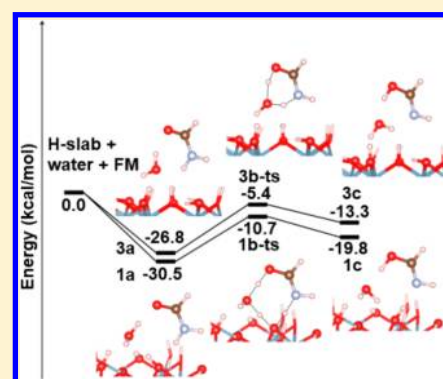
Effects of Water Molecules on Rearrangements of Formamide on the Kaolinite Basal (001) Surface

Huyen Thi Nguyen and Minh Tho Nguyen*

Department of Chemistry, University of Leuven, B-3001 Leuven, Belgium

S Supporting Information

ABSTRACT: The effects of kaolinite mineral surfaces on the unimolecular rearrangements of formamide (FM) were investigated using periodic density functional theory in conjunction with pseudopotential plane-wave approach. Surface hydroxyl groups covering the octahedral surface of kaolinite were found to play the role of catalysts in the transformations of FM. They induce a reduction of 31 kcal/mol on the energy barrier for formation of its isomer aminohydroxymethylene (AHM), which is close to the reduction amount calculated for water-catalyzed reactions. This suggests that the kaolinite octahedral surface exerts a catalytic effect similar to that of the water molecule. As the tetrahedral surface does not contain catalytic surface hydroxyl groups, only water-assisted FM transformation was therefore studied on this surface whose energy barrier amounts to ~ 17 kcal/mol. The combined effect of both water and kaolinite on FM rearrangements via triple hydrogen transfer reactions does not significantly lower the energy barriers, as compared to those of double hydrogen transfer reactions. The triple hydrogen transfer energy barriers amount to ~ 20 and ~ 36 kcal/mol, and the double ones are ~ 21 and ~ 40 kcal/mol for formation of formimic acid and AHM isomers, respectively. However, the energies of the systems in water-catalyzed channels lie below the available energies of the original reactants, and thus these channels are more favored than the water-free ones. With its multiple functions as both a supporting plate-form and a catalyst for FM reactions, kaolinite can thus be regarded as an important natural catalyst for prebiotic synthesis.



1. INTRODUCTION

Formamide (NH_2CHO , FM) has recently attracted great interest in the field of prebiotic syntheses.¹ FM is the simplest member of the amide functional group and a smallest stable molecule containing the four C, H, O, and N elements. It has been detected in comets,² some celestial bodies in the solar system,³ and interstellar medium.⁴ A particularly interesting characteristic of FM is its fragmentations forming a wide range of low molecular weight products, for example, HCN, H_2O , CO, and NH_3 .^{5,6} Hydrogen cyanide HCN is one of the most relevant prebiotic precursors because a variety of important biomolecules can be synthesized from its polymerization reactions.^{7–9} Formation of HCN from FM occurs in two main steps, namely (i) rearrangements of FM forming its isomers, formimic acid (NHCHOH , FA) and aminohydroxymethylene (NH_2COH , AHM) and (ii) dehydrations of FA or AHM. Without the presence of catalysts, the energy barriers of these steps were calculated in the range 19–50 kcal/mol for the first step and of 57–76 kcal/mol for the second step, depending on the methods employed.^{5,6,10,11} Following triplet excitation, the unimolecular rearrangement barrier of FM is significantly reduced as compared to the corresponding barrier in the ground singlet state.⁶ However, the high dehydration barrier of step ii in the triplet state results in a high overall barrier of ~ 51 kcal/mol for the whole process.⁶

Several theoretical studies have reported on bifunctional catalysts such as water or FM itself that turn out to efficiently lower the unimolecular rearrangement and dehydration barriers.^{10–13} Similar to the effect of triplet excitation, the presence of one or more water molecules also considerably reduces the rearrangement and dehydration barriers, which are now in the ranges 17–23 and 33–38 kcal/mol, respectively. However, the overall barriers of these water-assisted reactions remain slightly higher than that of the rate-determining step of reactions in the triplet state. A slightly lower overall barrier of ~ 48 kcal/mol was reported for self-catalyzed reactions by Wang et al.¹³ The energy barriers for steps i and ii are 26 and 19 kcal/mol, respectively (note that the levels of theory, DFT/B3LYP, used in this paper are not the same). Although there is significant reduction on the energy barrier of each step, the energy barriers with respect to water–FM and FM–FM reactant complexes in both water-assisted and self-catalyzed processes show little improvement as compared to the barriers for noncatalyzed cases. This rather limited reduction is due to the fact that water–FA/AHM or FA/AHM bimolecular complexes (reactant complexes for the dehydration step) lie much higher in energy than water–FM or FM–FM ones, and

Received: May 30, 2014

Revised: July 29, 2014

Published: July 29, 2014

that makes the energy barrier of the rate-determining step also high.

We recently reported a pathway for efficient formation of HCN/HNC from FM combining the advantages of water-assisted rearrangements, self-catalyzed dehydrations and mineral surfaces.¹⁴ With their multiple functional groups, mineral surfaces can connect both types of reactions and thus the routes involving bimolecular complexes from FM dimers with very high energy barriers can be avoided. The effects of sulfur-deficient defects and water on the rearrangement barriers of FM on the (100) surface of pyrite (FeS₂) were investigated.¹⁴ Because the reduction of FM rearrangement barrier was observed only in water-assisted reactions, it suggested that the pyrite surface induces no significant catalytic effect and thus its basic function is a plate-form for, or connecting bridge between the water-assisted rearrangements of FM and the self-catalyzed dehydrations of FA/AHM.

Besides metal sulfide groups of minerals, involvement of clay minerals in chemical evolution has also been extensively studied.^{15–21} The clay minerals can adsorb different species in the surrounding environment and protect them from degradation under harsh conditions of the early Earth.^{15,16} Their accumulations on the clay mineral surfaces could result in further reactions, which in turn lead to the formations of more complex molecules either with or without clay surface groups as catalysts.^{15–19} It was also proven that the clay molecules can offer protection for resulting biomolecule products.^{19,20}

Among different types of clay minerals, kaolinite has the highest adsorption affinity for biomolecules.²¹ Kaolinite has a 1:1 dioctahedral structure and a common chemical formula of Al₂Si₂O₅(OH)₄. Each kaolinite layer is parallel to the crystallographic (001) surface and has two connecting sheets via a plane of apical oxygen atoms, an octahedral AlO₆ sheet and a tetrahedral SiO₄ sheet (cf. Figure 1). Two adjacent layers

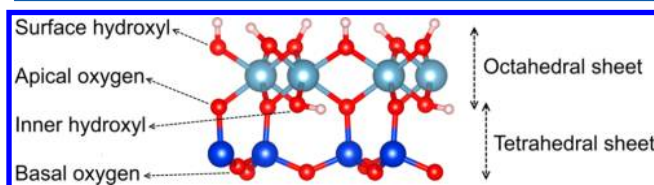


Figure 1. Structure of kaolinite showing octahedral sheet, tetrahedral sheet, inner and surface hydroxyl groups, and apical and basal oxygen atoms.

are bound by strong hydrogen bonds between surface hydroxyl groups on the octahedral side, and basal oxygen atoms on the tetrahedral side. Because of the presence of these flexible surface hydroxyl groups, polar molecules preferentially interact with the hydrophilic octahedral sheet rather than with the hydrophobic tetrahedral one.^{22–24}

In this context, we set out to investigate the possible catalytic function of kaolinite mineral in the reactivities of FM, in particular in HCN formation. We consider the adsorption of FM on the kaolinite basal (001) surfaces and its transformations and also assess the effect of water molecules on the adsorption process. We thus determine the extent of catalytic effects of both water molecules and kaolinite surfaces on the transformations of FM.

2. COMPUTATIONAL METHODS

Geometry optimizations are carried out to obtain fully relaxed structures of bulk and surfaces. All calculations are performed using the Vienna ab initio software package (VASP, version 4.6).^{25–27} Density functional theory (DFT) method²⁸ with the projected augmented wave (PAW) description^{29,30} of cores and the Perdew and Wang (PW91) functional³¹ for the exchange–correlation energy are employed. The valence electrons are described by a plane-wave basis set with a kinetic energy cutoff of 520 eV. For the bulk kaolinite, *k*-point sampling is performed with a 4 × 2 × 3 Monkhorst–Pack sampling grid.³² The ideal (001) surfaces of kaolinite are modeled by (2 × 1) slabs, which are cut from the fully optimized bulk structure. These slabs consist of one layer of kaolinite with two different exposed basal surfaces plotted in Figure 2: the octahedral surface **H-slab** and

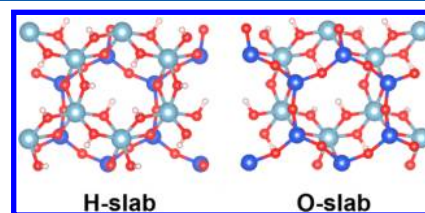


Figure 2. Structures of octahedral (**H-slab**) and tetrahedral (**O-slab**) surfaces of kaolinite.

the tetrahedral surface **O-slab**. Geometry optimizations of these bare slabs are carried out with 2 × 2 × 1 Monkhorst–Pack *k*-point sampling and the vacuum gap of ~10 Å above the kaolinite surface. A distance of 3 Å is added to the *c* lattice parameter when reactive species adsorb on the surfaces. The geometries of FM, its two tautomers (formimic acid (NHCHOH, FA) and aminohydroxymethylene (NH₂COH, AHM) and water are individually relaxed in a box of dimensions 20 Å × 20 Å × 20 Å at the same cutoff energy as bulk and slab calculations. All structures are allowed to fully relax without restraints. Transition state structures (TS) are obtained using the climbing image–nudged elastic band (CI–NEB) method.^{33,34}

Kaolinite bulk structures have been reported in many experimental and theoretical investigations.^{35–41} The low-temperature neutron powder diffraction structure data of kaolinite reported by Bish³⁶ (*a* = 5.1535 Å, *b* = 8.9419 Å, *c* = 7.3906 Å, α = 91.926°, β = 105.046°, γ = 89.797°) served as a basic input structure for our lattice optimization process, in which the cell lengths are varied while the cell angles are fixed. The resulting optimized lattice constants slightly differ from the experimental ones with a deviation of ~1.4%. Using this optimized bulk structure, we create the octahedral **H-slab** and tetrahedral **O-slab** surfaces with surface dimensions being 10.4 Å × 9.1 Å. The *c* lattice parameter is set to be 15.3 Å to ensure a ~10 Å vacuum gap between two adjacent periodic supercells. During the slab optimizations, all atoms are allowed to fully relax inside these fixed periodic supercells. The reactive species (FM and water) are then put on top of the optimized slabs in various positions to find suitable and stable molecule(s)–kaolinite adsorption complexes for FM transformations.

3. RESULTS AND DISCUSSION

3.1. Formamide on Octahedral and Tetrahedral Surfaces of Kaolinite. FM is found to adsorb on octahedral surface of kaolinite in perpendicular orientation. The most

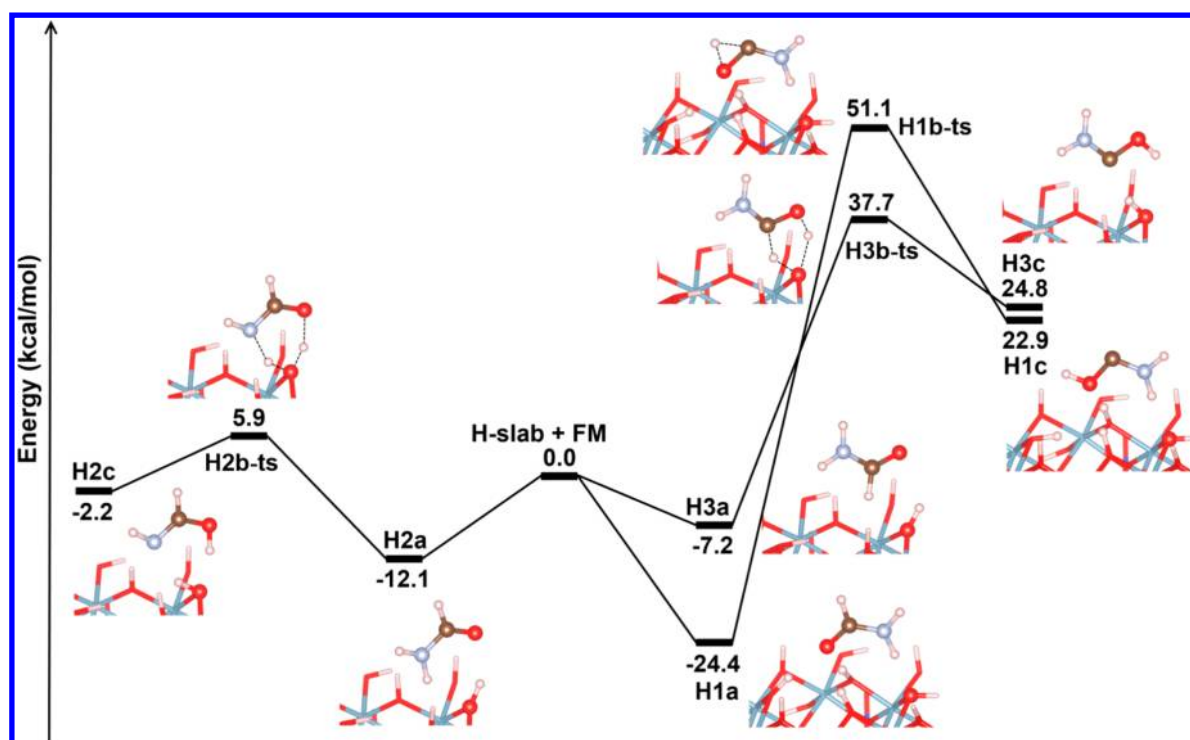


Figure 3. Schematic one-dimensional potential energy profiles illustrating the interconversions of **H1a**, **H2a**, and **H3a** complexes.

stable adsorption complex between FM and **H-slab** obtained from our calculations is **H1a**, characterized by the adsorption energy of -24.4 kcal/mol (by convention, a negative adsorption energy corresponds to a stable complex lying below the separated reactants). In complex **H1a**, four surface hydroxyl ($-\text{OH}$) groups are involved in the formation of hydrogen bonds (cf. Figure 3). The carbonyl oxygen atom acts as a proton acceptor and interacts with three surface $-\text{OH}$ groups. In the fourth hydrogen bond, the FM $-\text{NH}_2$ group acts as proton donor and the surface $-\text{OH}$ group as a proton acceptor. The $-(\text{H})\text{O}\cdots\text{HN}(\text{H})-$ bond with the bond distance of 1.81 Å is slightly stronger than the three $-\text{OH}\cdots\text{O}=\text{C}$ hydrogen bonds. In a recent report of Song et al.,⁴² the structure of the lowest FM-**H-slab** adsorption complex **Al-FA-1** is quite similar to that of **H1a**. However, there are only three hydrogen bonds between FM and the kaolinite surface in the **Al-FA-1** complex. The amino $-\text{NH}_2$ group of FM moves closer to the surface $-\text{OH}$ group, resulting in a shorter hydrogen bond of 1.77 Å. The carbonyl oxygen is thus too far away from the surface $-\text{OH}$ group, which lies in the plane of FM molecule to form hydrogen bond.

Two other adsorption complexes **H2a** and **H3a** are chosen for further investigation because their atomic arrangements could facilitate one-step FM transformations via double hydrogen transfer reactions. These two adsorption complexes have, however, only two weaker hydrogen bonds between FM and surface $-\text{OH}$ groups. As a result, **H2a** and **H3a** have much lower adsorption energies than **H1a**, being -12.1 and -7.2 kcal/mol, respectively. Opposite to the previous case where only FM has a bifunctional character, both the FM and surface $-\text{OH}$ group in **H2a** and **H3a** are amphoteric with the abilities to, in the mean time, donate and accept proton. The surface $-\text{OH}$ group acts as proton donor to the carbonyl oxygen and as proton acceptor to the carbonyl/ $-\text{NH}_2$ hydrogen of FM. In complex **H2a**, the hydrogen bond $-\text{OH}\cdots\text{O}=\text{C}$ is stronger than

$-(\text{H})\text{O}\cdots\text{HN}(\text{H})-$ with the former distance being 0.17 Å longer than the latter. Both hydrogen bonds in **H3a** are apparently weaker than those of **H2a**. However, in this case the $-\text{OH}\cdots\text{O}=\text{C}$ bond distance is 0.1 Å shorter than the $-(\text{H})\text{O}\cdots\text{HC}(\text{O})-$ value.

Schematic one-dimensional potential energy profiles are presented in Figure 3, illustrating the transformations of complexes **H1a** and **H3a** yielding the AHM-**H-slab** complex and of complex **H2a** forming the FA-**H-slab** complex. The AHM-**H-slab** complex **H1c** is formed from **H1a** via hydrogen transfer reaction, where a carbonyl hydrogen is transferred from carbon to oxygen. The two breaking bonds $\text{C}_{\text{FM}}\cdots\text{H}_{\text{FM}}$ and $\text{O}_{\text{FM}}\cdots\text{H}_{\text{FM}}$ in the transition structure **H1b-ts** have the bond distances of 1.29 and 1.19 Å, respectively. The energy barrier of ~ 76 kcal/mol of **H1a** rearrangement is, however, close to those of FM transformations on the ideal and defect (100) surfaces of pyrite, which amount to ~ 72 – 75 kcal/mol.¹⁴ Similar to adsorption for the pyrite surfaces, adsorption on the kaolinite octahedral surface obviously does not also affect significantly the energy barrier for FM transformation.

As mentioned above, the transformations of **H2a** and **H3a** are processed via double hydrogen transfer reactions. The corresponding transition structures follow the patterns of the corresponding adsorption complexes with the breaking of covalent bonds forming new hydrogen bonds, and the formations of new covalent bonds from previous hydrogen bonds. The transition structure **H2b-ts** has a six-membered cyclic shape, in which the surface $-\text{OH}$ group transfers its hydrogen atom to the carbonyl oxygen atom of FM, and at the same time forms a new bond with the released hydrogen atom of $-\text{NH}_2$ group. A five-membered ring is taking shape in the transition structure **H3b-ts** with the two transferred hydrogen atoms being the surface $-\text{OH}$ and carbonyl hydrogen atoms. Important geometrical parameters of transition structures **H2b-ts** and **H3b-ts** are listed in Table 1. According to these data, the

Table 1. Bond Distances (Å) of Breaking Bonds in Calculated Transition Structures H1b-ts, H2b-ts, H3b-ts, Hw2-1b-ts, Hw2-2b-ts, Hw2-3b-ts, Hw2-4b-ts, Ow3-1b-ts, and Ow3-2b-ts^a

	$C_{FM} \cdots H_{FM}$	$O_{FM} \cdots H_{FM}$					
H1b-ts	1.286	1.191					
	$O_{FM} \cdots H_s$	$H_s \cdots O_s$	$O_s \cdots H_{FM}$	$H_{FM} \cdots N_{FM}$	$H_{FM} \cdots C_{FM}$		
H2b-ts	1.496	1.069	1.063	1.589			
H3b-ts	1.081	1.573	1.314	1.344			
	$O_{FM} \cdots H_w$	$H_w \cdots O_w$	$O_w \cdots H_s$	$H_s \cdots O_s$	$O_s \cdots H_{FM}$	$H_{FM} \cdots N_{FM}$	$H_{FM} \cdots C_{FM}$
Hw2-1b-ts	1.185	1.267	1.232	1.227	1.231	1.361	
Hw2-2b-ts	1.055	1.485	1.056	1.525	1.298		1.463
	$O_{FM} \cdots H_w$	$H_w \cdots O_w$	$O_w \cdots H_{FM}$	$H_{FM} \cdots N_{FM}$	$H_{FM} \cdots C_{FM}$		
Hw2-3b-ts	1.092	1.401	1.228	1.302			
Hw2-4b-ts	1.015	1.746	1.285	1.336			
Ow3-1b-ts	1.285	1.183	1.156	1.400			
Ow3-2b-ts	1.187	1.283	1.183	1.510			

^aSubscripts “FM”, “w”, and “s” represent atoms of FM, water, and kaolinite surfaces, respectively.

hydrogen transfer from the surface –OH group to the carbonyl oxygen of FM in H2b-ts is in the beginning state whereas the other one is already in the final state of the transfer process, with the bond distances of $H_s \cdots O_s$ and $O_s \cdots H_{FM}$ being 1.07 and 1.06 Å, respectively. The two hydrogen transfer processes in H3b-ts are also different with nearly complete H_s transfer and H_{FM} being in the middle of the process.

AHM–H-slab complex H3c is generated via a barrier height of 45 kcal/mol, which is now 31 kcal/mol lower than the energy barrier for H1a rearrangement. Such a reduction in energy barrier due to the catalytic effect of the octahedral surface of kaolinite is comparable to that of the water-assisted rearrangement both in the gas phase^{10–12} and on pyrite surfaces.¹⁴ This result clearly suggests that the kaolinite octahedral surface, specifically the surface –OH groups, could behave as a catalyst equally as good as water for FM rearrangements in nonaqueous environments. It should be noted that the catalytic effect of the kaolinite octahedral surface is limited to the reduction of the transformation barrier. The kaolinite surface, however, does not greatly change the relative stabilities between the FM isomers.

Compared to the formation of AHM–H-slab complex, that of FA–H-slab complex H2c is connected via a transition structure with much lower relative energy. The corresponding barrier height of this double hydrogen transfer reaction is only 18 kcal/mol. Another advantage of H2c formation over H3c formation is that the former product is much more stable than the latter one (the reaction being more exothermic), which, as expected, results in a lower overall energy barrier for HCN formation from FM in combination with subsequent self-catalyzed dehydration.

Different FM–O-slab complexes having two hydrogen bonds between FM and the tetrahedral surface were reported in a recent paper.⁴² The most stable one is Si-FA-1 with adsorption energy being –10.2 kcal/mol. From our periodic supercell calculations, another adsorption complex O1a is found (Figure 4) with an adsorption energy of –8.5 kcal/mol. The FM molecule is oriented parallel to the tetrahedral surface with the carbonyl oxygen pointing toward Si atom. Due to this

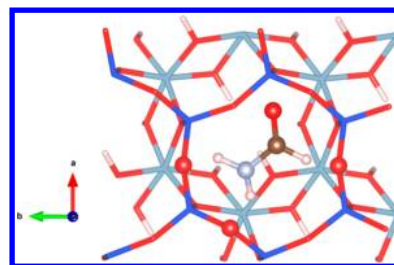


Figure 4. Structure of formamide adsorbed on the tetrahedral surface of kaolinite.

parallel arrangement, three basal oxygen atoms are involved in the hydrogen bonds with FM hydrogen atoms in this complex. However, addition of one more hydrogen bond is accompanied by an increase in repulsion interaction between the molecule and the surface, rendering the complex less stable. Forcing the carbonyl oxygen down onto the tetrahedral hole to interact with inner –OH group is thus a disfavored action. Because double hydrogen transfer reaction cannot originate from the O1a complex, FM rearrangements from FM–O-slab complexes will not be further investigated.

3.2. Formamide on Octahedral and Tetrahedral Surfaces of Kaolinite with the Presence of a Water Molecule. In this section, the effects of water and kaolinite mineral surfaces are examined both separately and collectively. We first determine several adsorption complexes between water molecule and the two basal surfaces of kaolinite. The FM molecule is then added to the water–surface complexes in specific orientations that facilitate FM rearrangements via double or triple hydrogen transfer reactions.

Water adsorption on kaolinite surfaces has previously been studied by means of grand canonical Monte Carlo simulations,²³ DFT calculations using a plane-wave pseudopotential approach,⁴¹ and molecular dynamics simulations.^{39,43,44} It has been proven that water preferentially adsorbs on 3-fold hollow sites, which are situated in the middle of Al hexagonal pattern, with the adsorption energy being in the range –13 to –15 kcal/mol.^{41,44}

Structures of water–H-slab and water–O-slab complexes are presented in Figures S1 and S2 in the Supporting Information. Water adsorbs perpendicularly to the octahedral surface, whereas on the tetrahedral surface, the molecular plane of water forms a smaller angle with the surface. In the latter case, the two hydrogen atoms are pointed toward the basal oxygen atoms and the oxygen atom tends to move farther from the surface.

In the most stable water–H-slab complex Hw1, water adsorbs on a 3-fold hollow site with water oxygen situated on top of Al position with the adsorption energy of –18.9 kcal/mol. Three hydrogen bonds are thus formed between FM and surface –OH groups with bond distances of 1.89, 2.00, and 2.09 Å. The water molecule acts in this case as a proton donor in the strongest hydrogen bond and as a proton acceptor in the others. In the second water–H-slab adsorption complex Hw2, the water molecule is located near the middle point of Al hexagonal rings and has a slightly smaller interaction energy of –14.4 kcal/mol, which is in good agreement with previously reported values.^{41,44} In this complex, water donates hydrogen making a $O \cdots H$ hydrogen bond of 1.92 Å, and accepts three other hydrogen bonds with $O \cdots H$ bond distances of 1.83, 1.86, and 2.58 Å from surface –OH groups. The weakest hydrogen bond in Hw2 is formed between water and the surface –OH

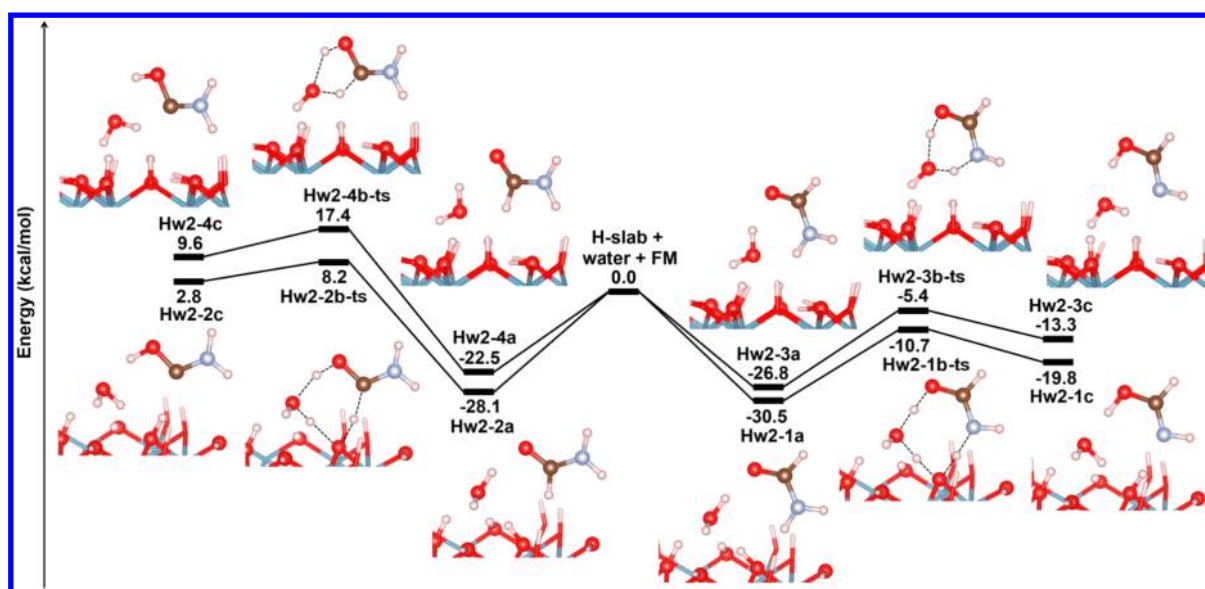


Figure 5. Schematic one-dimensional potential energy profiles illustrating the interconversions of Hw2-1a, Hw2-2a, Hw2-3a, and Hw2-4a complexes.

group, which lies on the water molecular plane. It should be noted that this hydrogen bond complex was not observed in previous DFT study, which reported only the formation of oxygen atom of water giving two hydrogen bonds with surface —OH group.⁴¹

Interaction between water and the tetrahedral surface turns out to be very weak. The adsorption energies of **Ow1** and **Ow2** amount to only -2.2 and -1.4 kcal/mol, respectively (cf. Figure S2 of the Supporting Information). In **Ow1**, two hydrogen atoms of water form two hydrogen bonds with O–H bonds of 2.12 and 2.54 Å with two adjacent basal oxygen atoms. The two latter atoms are located close to the molecular plane of adsorbed water with dihedral angles $\text{H}_w\text{—O}_w\text{—H}_w\text{—O}_s$ of $\sim 9^\circ$ (the subscripts “w” and “s” stand for atoms of water and the surface, respectively). This orientation is also observed in **Ow2** in which water and two opposite basal oxygen atoms lying on a plane normal to the surface. The two hydrogen bonds between water and surface oxygen atoms in **Ow2** are 2.32 and 2.54 Å.

FM orientation on the water–surface complexes is chosen in such a way to generate structures in which FM can undergo rearrangements to form FA/AHM isomers via double/triple hydrogen transfer reactions. Formation of the latter isomers is a necessary step for subsequent dehydration reactions. Because the triple hydrogen transfer reactions are successfully calculated only for the complexes between FM and **Hw2**, the schematic one-dimensional potential energy profile illustrating their interconversions is presented here in Figure 5. The results of FM–**Hw1** complexes can be found in Figure S3 in the Supporting Information.

Let us now consider the four different FM–**Hw2** complexes including the **Hw2-1a**, **Hw2-2a**, **Hw2-3a**, and **Hw2-4a**. Among these complexes, the two more stable **Hw2-1a** and **Hw2-2a** characterized by large adsorption energies of -30.5 and -28.5 kcal/mol, respectively, are involved in triple hydrogen transfer reactions. The two less stable complexes **Hw2-3a** and **Hw2-4a** are involved in double hydrogen transfer reactions. In the two former complexes, FM donates one hydrogen bond to the surface —OH group and accepts one hydrogen bond from water. Water also forms two hydrogen bonds with the surface —OH groups, one of which is the same group that accepts

hydrogen bond from FM. This specific arrangement of FM, water and the surface —OH group facilitate a triple hydrogen transfer relay, in which FM transfers one hydrogen atom to the surface —OH group and, at the same time, forms a new bond with one hydrogen atom from water. In double hydrogen transfers of **Hw2-3a** and **Hw2-4a**, FM transfers one hydrogen atom to water and receives a hydrogen atom of water yielding a new H-bond. These hydrogen transfer processes are indicated by black dash line in Figure 5.

The lengths of these broken bonds in the transition structures **Hw2-1b-ts**, **Hw2-2b-ts**, **Hw2-3b-ts**, and **Hw2-4b-ts** are listed in Table 1. Similar to hydrogen transfers in transition structures **H2b-ts** and **H3b-ts**, the hydrogen transfers in these four transition structures in general have different degrees of advancement. The transfers of H_w and H_s in **Hw2-2b-ts**, and H_w in **Hw2-3b-ts** and **Hw2-4b-ts** are nearly complete, with the bond distances of the breaking bonds being close to the values of the corresponding covalent bonds in the products. These bonds are thus virtually formed. On the contrary, the transferred hydrogen atoms in other hydrogen transfer processes lie in the middle of the two heavier atoms.

Both types of reactions clearly yield much lower energy barriers than the corresponding unimolecular transformations. Formations of FA complexes from **Hw2-1a** and **Hw2-3a** have energy barriers of 19.8 and 21.4 kcal/mol, respectively, whereas AHM formations from **Hw2-2a** and **Hw2-4a** are associated barrier heights of 36.3 and 39.9 kcal/mol, respectively. As we can see, the energy barriers of double and triple hydrogen transfer reactions are quite close to each other as well as to the energy barriers of **H2a** and **H3a** reactions. This result suggests that the individual catalytic effects of hydroxylated octahedral surface and of water on FM rearrangements are similar. Furthermore, it also shows that combination of catalytic effects of both surface and water does not result in sensitive improvement in lowering the energy barriers. The triple hydrogen transfer barriers are only $\sim 2\text{--}4$ kcal/mol lower than those involving double hydrogen transfers. However, the relative energies of the transition structures **Hw2-1b-ts** and **Hw2-3b-ts** are lower than the available energies of the original reactants. This suggests that the isomerization reactions can

proceed more easily via water-catalyzed channels than water-free channels.

Among the two possible arrangements of FM on the water–O-slab complexes, the complex **Ow1–1a** with suitable arrangement for the formation of FA via double hydrogen transfer reaction has the lowest adsorption energy being -9.0 kcal/mol (Figure 6). This is due to the fact that the water

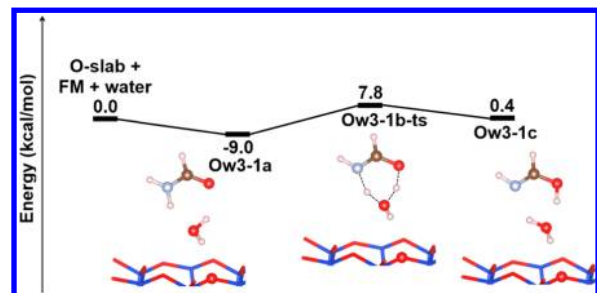


Figure 6. Schematic one-dimensional potential energy profile illustrating the interconversion of **Ow1–1a** complex.

oxygen atom in **Ow1–1a** moves away from the surface following interaction with FM, and as a consequence, the repulsive interaction is reduced. Double hydrogen transfer reaction from **Ow1–1a** has the energy barrier of ~ 17 kcal/mol, which is lower than the corresponding values of **H2a**, **Hw2–1a**, and **Hw2–3a** reactions.

4. CONCLUDING REMARKS

The effects of kaolinite mineral surfaces on the rearrangements of FM were investigated in the present theoretical study using periodic density functional theory in conjunction with the pseudopotential plane-wave approach. Surface hydroxyl groups covering the octahedral surface of kaolinite were found to play the role of catalysts in the transformations of FM. Formation of the isomer AHM from FM via double hydrogen transfer reaction with the surface hydroxyl group is associated with an energy barrier of ~ 45 kcal/mol, being ~ 31 kcal/mol lower than that of the uncatalyzed reaction. The fact that this amount of energy reduction is close to the values of water-catalyzed AHM formation both in the gas phase and on the previously reported solid surface, suggests that kaolinite octahedral surface has a comparable catalytic effect as water molecules, and thereby can effectively catalyze FM rearrangements in nonaqueous environments. Adsorption of FM on the tetrahedral surface does not give rise to complexes with suitable preassociation structures for double hydrogen transfer reactions. Therefore, lower energy barrier FM transformation reactions on this surface can only be effective when water adsorbs on the surface and subsequently acts as catalyst. The water-assisted FA formation on the tetrahedral surface has a lower energy barrier of ~ 17 kcal/mol.

The catalytic effect of kaolinite surface on FM isomerizations in the presence of one water molecule was also studied. The collective effect of both water and kaolinite on FM rearrangements does not significantly improve the catalytic process. The energy barriers of triple hydrogen transfer reactions are only 2–4 kcal/mol lower than those of double hydrogen transfer reactions. The former values are 20 and 36 kcal/mol, and the latter values amount to 21 and 40 kcal/mol for FA and AHM formations, respectively. However, in the presence of water molecule(s), the energy levels of the transition structures are well below the available energies of the original reactants, and

thus these reaction channels become more favored than the water-free channels.

In conclusion, kaolinite functions most likely as both a supporting plate-form and a catalyst for FM reactions. The adsorbed FM molecule can take part in low energy barrier rearrangements via double/triple hydrogen transfer reactions, yielding FA and AHM on the surfaces. Bimolecular complexes formed from these latter molecules are in turn reactants for subsequent self-catalyzed dehydrations forming the important prebiotic precursors HCN/HNC.

■ ASSOCIATED CONTENT

Supporting Information

Structures of water–H-slab and water–O-slab adsorption complexes and schematic one-dimensional potential energy profiles illustrating rearrangements of FM–**Hw1**, FM–**Ow1**, and FM–**Ow2** complexes. This material is available free of charge via the Internet at <http://pubs.acs.org>.

■ AUTHOR INFORMATION

Corresponding Author

*M. T. Nguyen. E-mail: minh.nguyen@chem.kuleuven.be.

Notes

The authors declare no competing financial interest.

■ ACKNOWLEDGMENTS

We are indebted to the KU Leuven Research Council (GOA and IDO programs) for continuing support. H.T.N. receives a doctoral scholarship from an interdisciplinary research project (IDO-2011) of KU Leuven on Exoplanets.

■ REFERENCES

- (1) Saladino, R.; Crestini, C.; Pino, S.; Costanzo, G.; Di Mauro, E. Formamide and the Origin of Life. *Phys. Life Rev.* **2012**, *9*, 84–104.
- (2) Despois, D.; Crovisier, J.; Bockelee-Morvan, D.; Biver, N. Comets and Prebiotic Chemistry: The Volatile Component. *Eur. Space Agency, [Spec. Publ.], SP* **2002**, *518*, 123–127.
- (3) Parnell, J.; Baron, M.; Lindgren, P. Potential for Irradiation of Methane to Form Complex Organic Molecules in Impact Craters: Implications for Mars, Titan and Europa. *J. Geochem. Explor.* **2006**, *89*, 322–325.
- (4) Solomon, P. M. Interstellar Molecules. *Phys. Today* **1973**, *26*, 32–40.
- (5) Nguyen, V. S.; Abbott, H. L.; Dawley, M. M.; Orlando, T. M.; Leszczynski, J.; Nguyen, M. T. Theoretical Study of Formamide Decomposition Pathways. *J. Phys. Chem. A* **2011**, *115*, 841–851.
- (6) Nguyen, H. T.; Nguyen, V. S.; Trung, N. T.; Havenith, R. W. A.; Nguyen, M. T. Decomposition Pathways of the Neutral and Protonated Formamide in Some Lower-Lying Excited States. *J. Phys. Chem. A* **2013**, *117*, 7904–7917.
- (7) Voet, A. B.; Schwartz, A. W. Uracil Synthesis Via HCN Oligomerization. *Origins Life Evol. Biospheres* **1982**, *12*, 45–49.
- (8) Ferris, J. P.; Hagan, W. J. HCN and Chemical Evolution - the Possible Role of Cyano Compounds in Prebiotic Synthesis. *Tetrahedron* **1984**, *40*, 1093–1120.
- (9) Roy, D.; Schleyer, P. v. R., Chemical Origin of Life: How do Five HCN Molecules Combine to form Adenine under Prebiotic and Interstellar Conditions. In *Quantum Biochemistry*; Wiley-VCH Verlag GmbH & Co. KGaA: Berlin, 2010; pp 197–217.
- (10) Wang, X. C.; Nichols, J.; Feyereisen, M.; Gutowski, M.; Boatz, J.; Haymet, A. D. J.; Simons, J. Ab initio Quantum Chemistry Study of Formamide-Formamidic Acid Tautomerization. *J. Phys. Chem.* **1991**, *95*, 10419–10424.

- (11) Wang, J.; Gu, J.; Nguyen, M. T.; Springsteen, G.; Leszczynski, J. From Formamide to Purine: An Energetically Viable Mechanistic Reaction Pathway. *J. Phys. Chem. B* **2013**, *117*, 2314–2320.
- (12) Nguyen, V. S.; Orlando, T. M.; Leszczynski, J.; Nguyen, M. T. Theoretical Study of the Decomposition of Formamide in the Presence of Water Molecules. *J. Phys. Chem. A* **2013**, *117*, 2543–2555.
- (13) Wang, J.; Gu, J. D.; Nguyen, M. T.; Springsteen, G.; Leszczynski, J. From Formamide to Purine: A Self-Catalyzed Reaction Pathway Provides a Feasible Mechanism for the Entire Process. *J. Phys. Chem. B* **2013**, *117*, 9333–9342.
- (14) Nguyen, H. T.; Nguyen, M. T. Effects of Sulfur-Deficient Defect and Water on Rearrangements of Formamide on Pyrite (100) Surface. *J. Phys. Chem. A* **2014**, *118*, 4079–4086.
- (15) Bernal, J. D. The Physical Basis of Life. *Proc. Phys. Soc. A* **1949**, *62*, 537.
- (16) Paecht-Horowitz, M. Clays as Possible Catalysts for Peptide Formation in the Prebiotic Era. *Origins Life* **1976**, *7*, 369–381.
- (17) Rao, M.; Odom, D. G.; Oro, J. Clays in Prebiological Chemistry. *J. Mol. Evol.* **1980**, *15*, 317–331.
- (18) Saladino, R.; Crestini, C.; Costanzo, G.; Negri, R.; Di Mauro, E. A Possible Prebiotic Synthesis of Purine, Adenine, Cytosine, and 4(3H)-Pyrimidinone from Formamide: Implications for the Origin of Life. *Bioorg. Med. Chem.* **2001**, *9*, 1249–1253.
- (19) Hashizume, H. *Role of Clay Minerals in Chemical Evolution and the Origins of Life*; InTech: Rijeka, Croatia, 2012; p 312.
- (20) Franchi, M.; Bramanti, E.; Bonzi, L. M.; Orioli, P. L.; Vettori, C.; Gallori, E. Clay-Nucleic Acid Complexes: Characteristics and Implications for the Preservation of Genetic Material in Primeval Habitats. *Origins Life Evol. Biospheres* **1999**, *29*, 297–315.
- (21) Cai, P.; Huang, Q. Y.; Zhang, X. W. Interactions of DNA with Clay Minerals and Soil Colloidal Particles and Protection against Degradation by DNase. *Environ. Sci. Technol.* **2006**, *40*, 2971–2976.
- (22) Tunega, D.; Bencko, L.; Haberhauer, G.; Gerzabek, M. H.; Lischka, H. Ab initio Molecular Dynamics Study of Adsorption Sites on the (001) Surfaces of 1:1 Dioctahedral Clay Minerals. *J. Phys. Chem. B* **2002**, *106*, 11515–11525.
- (23) Croteau, T.; Bertram, A. K.; Patey, G. N. Adsorption and Structure of Water on Kaolinite Surfaces: Possible Insight into Ice Nucleation from Grand Canonical Monte Carlo Calculations. *J. Phys. Chem. A* **2008**, *112*, 10708–10712.
- (24) Scott, A. M.; Dawley, M. M.; Orlando, T. M.; Hill, F. C.; Leszczynski, J. Theoretical Study of the Roles of Na⁺ and Water on the Adsorption of Formamide on Kaolinite Surfaces. *J. Phys. Chem. C* **2012**, *116*, 23992–24005.
- (25) Kresse, G.; Furthmüller, J. Efficiency of ab-initio Total Energy Calculations for Metals and Semiconductors using a Plane-Wave Basis Set. *Comput. Mater. Sci.* **1996**, *6*, 15–50.
- (26) Kresse, G.; Furthmüller, J. Efficient Iterative Schemes for ab initio Total-Energy Calculations using a Plane-Wave Basis Set. *Phys. Rev. B* **1996**, *54*, 11169–11186.
- (27) Kresse, G.; Hafner, J. Ab-Initio Molecular-Dynamics Simulation of the Liquid-Metal Amorphous-Semiconductor Transition in Germanium. *Phys. Rev. B* **1994**, *49*, 14251–14269.
- (28) Kohn, W.; Sham, L. J. Self-Consistent Equations Including Exchange and Correlation Effects. *Phys. Rev. A* **1965**, *140*, 1133–1138.
- (29) Blochl, P. E. Projector Augmented-Wave Method. *Phys. Rev. B* **1994**, *50*, 17953–17979.
- (30) Kresse, G.; Joubert, D. From ultrasoft pseudopotentials to the projector augmented-wave method. *Phys. Rev. B* **1999**, *59*, 1758–1775.
- (31) Perdew, J. P.; Wang, Y. Accurate and Simple Analytic Representation of the Electron-Gas Correlation-Energy. *Phys. Rev. B* **1992**, *45*, 13244–13249.
- (32) Pack, J. D.; Monkhorst, H. J. Special Points for Brillouin-Zone Integrations - Reply. *Phys. Rev. B* **1977**, *16*, 1748–1749.
- (33) Mills, G.; Jonsson, H.; Schenter, G. K. Reversible Work Transition-State Theory - Application to Dissociative Adsorption of Hydrogen. *Surf. Sci.* **1995**, *324*, 305–337.
- (34) Jónsson, H.; Mills, G.; Jacobsen, K. W. Nudged Elastic Band Method for Finding Minimum Energy Paths of Transition. In *Classical and Quantum Dynamics in Condensed Phase Simulations*; World Scientific: Singapore, 1998; pp 385–404.
- (35) Young, R. A.; Hewat, A. W. Verification of the Triclinic Crystal-Structure of Kaolinite. *Clays Clay Miner.* **1988**, *36*, 225–232.
- (36) Bish, D. L. Rietveld Refinement of the Kaolinite Structure at 1.5-K. *Clays Clay Miner.* **1993**, *41*, 738–744.
- (37) Frost, R. L. The Structure of the Kaolinite Minerals - A FT-Raman Study. *Clay Miner.* **1997**, *32*, 65–77.
- (38) Neder, R. B.; Burghammer, M.; Grasl, T.; Schulz, H.; Bram, A.; Fiedler, S. Refinement of the Kaolinite Structure from Single-Crystal Synchrotron Data. *Clays Clay Miner.* **1999**, *47*, 487–494.
- (39) Warne, M. R.; Allan, N. L.; Cosgrove, T. Computer Simulation of Water Molecules at Kaolinite and Silica Surfaces. *Phys. Chem. Chem. Phys.* **2000**, *2*, 3663–3668.
- (40) Tosoni, S.; Doll, K.; Ugliengo, P. Hydrogen Bond in Layered Materials: Structural and Vibrational Properties of Kaolinite by a Periodic B3LYP Approach. *Chem. Mater.* **2006**, *18*, 2135–2143.
- (41) Hu, X. L.; Michaelides, A. Water on the Hydroxylated (001) Surface of Kaolinite: From Monomer Adsorption to a Flat 2D Wetting Layer. *Surf. Sci.* **2008**, *602*, 960–974.
- (42) Song, K. H.; Wang, X.; Qian, P.; Zhang, C.; Zhang, Q. Theoretical Study of Interaction of Formamide with Kaolinite. *Comput. Theor. Chem.* **2013**, *1020*, 72–80.
- (43) Smirnov, K. S.; Bougeard, D. A Molecular Dynamics Study of Structure and Short-Time Dynamics of Water in Kaolinite. *J. Phys. Chem. B* **1999**, *103*, 5266–5273.
- (44) Tunega, D.; Gerzabek, M. H.; Lischka, H. Ab initio Molecular Dynamics Study of a Monomolecular Water Layer on Octahedral and Tetrahedral Kaolinite Surfaces. *J. Phys. Chem. B* **2004**, *108*, 5930–5936.